LANGMUIR

pubs.acs.org/Langmuir Article

Layer-by-Layer Nanoarchitectonics Using Protein−Polyelectrolyte Complexes toward a Generalizable Tool for Protein Surface Immobilization

Cédric Vranckx,* Laure Lambricht, Véronique Préat, Olivier Cornu, Christine Dupont-Gillain,* and Aurélien vander Straeten

Cite This: *Langmuir* 2022, 38, 5579−5589 Read Online

ABSTRACT: Layer-by-layer (LbL) self-assembly is an attractive method for the immobilization of macromolecules at interfaces. Integrating proteins in LbL thin films is however challenging due to their polyampholyte nature. Recently, we developed a method to integrate lysozyme into multilayers using protein−polyelectrolytes complexes (PPCs). In this work, we extended this method to a wide range of protein−polyelectrolyte combinations. We demonstrated the robustness and versatility of PPCs as building blocks. LL-37, insulin, lysozyme, and glucose oxidase were complexed with alginate, poly(styrenesulfonate), heparin, and poly(allylamine hydrochloride). The resulting PPCs were then LbL self-assembled with chitosan, PAH, and heparin. We demonstrated that multilayers built with PPCs are thicker compared to the LbL self-assembly of bare protein molecules. This is attributed to the higher mass of protein in the multilayers and/or the more hydrated state of the assemblies. PPCs enabled the self-assembly of proteins that could otherwise not be LbL assembled with a PE or with another protein. Furthermore, the results also show that LbL with PPCs enabled the construction of multilayers combining different proteins, highlighting the formation of multifunctional films. Importantly, we show that the adsorption behavior and thus the multilayer growth strongly depend on the nature of the protein and polyelectrolyte used. In this work, we elaborated a rationale to help and guide the use of PPCs for protein LbL assembly. It will therefore be beneficial to the many scientific communities willing to modify interfaces with hard-to-immobilize proteins and peptides.

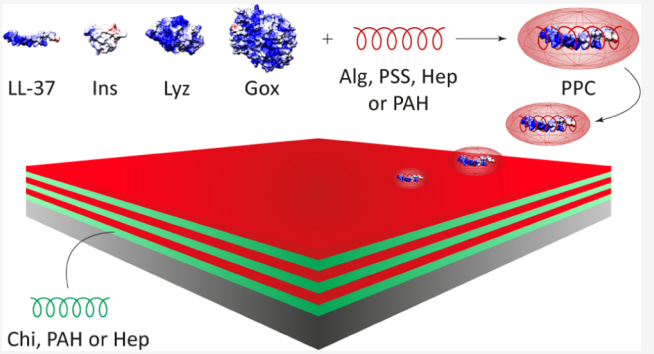

INTRODUCTION

The immobilization of active biomacromolecules is topical in biosensing,[1,2] heterogeneous biocatalysis,[3,4] drug delivery,[5,6] and tissue engineering.[7,8] In this respect, a myriad of methods were developed to functionalize material surfaces with proteins and peptides.[9] However, protein immobilization is far from straightforward because for most applications, proteins should retain their bioactivity. Hence, their immobilization should protect them from denaturation and degradation.

The simplest approach to immobilize proteins is to use their tendency to spontaneously adsorb on surfaces.[10] However, in addition to affecting the protein functionality through conformation[11,12] and orientation changes,[13,14] spontaneous protein adsorption can be reversible and the amount is often limited to a monolayer.[15−17] To limit protein desorption, chemical grafting has been used routinely. This method is not straightforward to implement since the surface must bear functional groups reacting with the protein. Moreover, chemical grafting might result in a loss of bioactivity caused by protein denaturation or reaction with the functional groups.[10,18,19] Finally, the adsorbed amount is also limited to a monolayer. Spontaneous adsorption and covalent grafting thus present major drawbacks when it comes to the immobilization of large amounts of bioactive proteins. Therefore, developing a versatile immobilization method without loss of protein activity is topical.

In 1992, Decher et al. demonstrated that polyelectrolyte multilayers (PEMs) can be constructed via a so-called layer-by-layer (LbL) self-assembly, i.e., by alternating the deposition of oppositely charged polyelectrolyte (PE) layers.[20,21] At each PE adsorption step, the surface charge is overcompensated, which allows the adsorption of the next layer of material. This results in the formation of a multilayer whose thickness can be precisely controlled by the number of adsorption steps.[22]

Received: January 24, 2022
Revised: April 13, 2022
Published: April 28, 2022

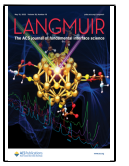

https://doi.org/10.1021/acs.langmuir.2c00191
Langmuir 2022, 38, 5579−5589

Though the latter mechanism is believed to drive PEM growth, other forces such as hydrophobic interactions and hydrogen bonding also participate in the assembly.[23,24] One of the major advantages of LbL assembly is that it is achievable under soft conditions, i.e., in aqueous solutions at room temperature, and it is versatile toward surface geometry and chemistry.[24] Therefore, the LbL assembly method has considerable potential for developing biofunctionalized materials with a great variety of architectures.[25]

Since Decher et al.'s first report, the LbL method has been extended to a wide range of deposited materials[22] such as clay minerals,[26,27] viruses,[28] dendrimers,[29,30] gold colloids,[31] silica particles,[32] and proteins.[33−35] Interestingly, this versatile method enables the assembly of multicomponent protein films, which open a way to construct multifunctional systems.[36] This is topical for various fields of research such as biomaterials, drug release, tissue engineering, and regenerative medicine. Importantly, proteins, peptides, and enzymes embedded in PEMs can also find applications in continuous flow chemistry and biocatalysis, as illustrated by the use of localized enzyme-assisted self-assembly (LEASA).[37−40] While the surface protein immobilization is crucial, their alternate adsorption with a PE in LbL fashion is not straightforward. Indeed, while PEs have a homogeneous charge distribution and are flexible macromolecules, proteins are polyampholytes with various degrees of charge anisotropy and a low conformational entropy. Hence, depending on the protein, PE, pH, and ionic strength (I) used for assembly, the multilayer may fail to grow.[41] The lack of charge overcompensation by the protein layer, i.e., the repulsion between the PE that is further adsorbed and the protein patches of the same charge, is believed to be the major cause of this failure.[42] The ineffective LbL assembly of the highly positively charged lysozyme (Lyz) with poly(methacrylic acid) at pH 8.4 was, for example, reported.[43] In this context, finding ways to circumvent the current limitations of protein LbL assembly with PEs is paramount.[34]

In 1996, Ariga et al. established that the LbL assembly of nonflexible molecules, such as proteins and organic dyes, is enhanced when they are premixed with linear polyions.[44] In 2001, Jin et al. found that the LbL formation of catalase microcrystals coated with poly(styrenesulfonate) (PSS) and assembled with poly(allylamine hydrochloride) (PAH) resulted in films with a better preserved enzymatic activity and a mass that was 1 order of magnitude higher than the ones obtained with uncoated catalase crystals.[45] However, this method requires protein crystals which limits its wide use. With a view to further facilitate the use of the LbL method for protein immobilization, protein−polyelectrolyte complexes (PPCs)[46,47] were recently introduced by our group as building blocks for the LbL assembly.[48,49] It was demonstrated that the PE corona of the PPCs standardizes the charge of the protein. The result is an LbL growth that is independent of the protein surface charge. This was shown for Lyz complexation with PSS and its subsequent LbL assembly with PAH.[49] Compared to the classical LbL assembly of bare Lyz, the PPCs-based self-assembly was shown to immobilize protein that has 75% more enzymatic activity.[48,49]

However, while PPCs have shown great potential to facilitate protein LbL assembly and maintain a high level of bioactivity, only one protein has been used to date, and the suggested versatility of PPCs remains theoretical. The objective of this work is to investigate whether PPCs can be used to immobilize a wide range of proteins and peptides, in combination with various PEs, using the LbL method. LL-37, insulin (Ins), Lyz, and glucose oxidase (Gox) were chosen because they are involved in different biomedical and biotechnological applications. These proteins were first complexed with an oppositely charged PE, i.e., alginate (Alg), PSS, heparin (Hep), and PAH. The resulting PPCs were then assembled with a second PE, i.e., chitosan (Chi), PAH, and Hep to form [PE-PPCs] multilayers. LL-37 is a human antimicrobial peptide of 37 amino acids, of 4.5 kDa, with an isoelectric point (IEP) of 11. It stimulates wound healing and angiogenesis and fights infections.[50,51] Ins is a peptide hormone of 5.8 kDa, with an IEP of 5.6, that regulates glycemia and that is used as a treatment for Type I diabetes. Lyz is an antimicrobial globular enzyme of 14.3 kDa, with an IEP of 11.1. It acts against some Gram-positive bacteria, through hydrolyzation of glycosidic bonds of peptidoglycans.[52,53] Gox is an enzyme of 66 kDa, with an IEP of 5.2, that catalyzes the oxidation of glucose. It is commonly used for the detection of blood glucose concentration.[54] The use of natural PEs is attractive for biomedical applications because they are usually biocompatible, biodegradable, and/or nontoxic. Alg is a polysaccharide naturally present in brown seaweed cell walls, with residues featuring a pK_a of 3.38 and 3.65.[55] It has become one of the most important biomaterials for regenerative medicine applications.[56,57] It is a weak polyacid due to its carboxyl groups. Hep is a glycosaminoglycan, used as an antithrombotic drug, which has the highest negative charge density of any known biological polyanion due to the presence of one carboxyl and three sulfonate groups per dimer.[58] Chi is a polysaccharide derived from chitin. This weak polycation, with an intrinsic pK_a varying from 6.46 to 7.32, depending on the degree of acetylation,[59] can be used for its antibacterial activity.[60] More generally, the use of biodegradable PEs can also be advantageous to promote the release of proteins from the multilayers and achieve controlled delivery of active ingredients.[61] In addition to natural PEs, synthetic PEs, i.e., PSS, and PAH are also used to study the formation of PPCs and further LbL assembly. [PAH-PSS] multilayers are indeed one of the most documented PEMs.[22] PSS is a strong polyanion, due to its sulfonate groups, whereas PAH is a weak polycation with a pK_a estimated to be between 8 and 9.[62]

PPCs were first fabricated, and their formation was evaluated by measuring the optical density of the solution. Then, the PPCs were LbL assembled with PEs and the multilayer growth was evaluated using quartz crystal microbalance with dissipation monitoring (QCM-D). The resulting multilayered films were compared to the ones obtained by the alternate assembly of bare proteins with PEs, i.e., the classical LbL method.

EXPERIMENTAL SECTION

Materials. LL-37 (Proteogenix, Schiltigheim, France), human Ins (Sigma-Aldrich, Steinheim, Germany), Lyz (Sigma-Aldrich, Steinheim, Germany), and Gox from *Aspergillus niger* (Sigma-Aldrich, Steinheim, Germany) were the selected proteins. Sodium Alg, M_W <75,000 g mol^{-1}, (Pronova UP VLVM, NovaMatrix, Norway), low molar mass PSS, M_W = 7540 g mol^{-1}, (Scientific Polymer, Ontario), and Hep sodium, 5000 I.E. mL^{-1}, (B. Braun, Melsungen, Germany), were used as polyanions. Chi, M_W = 10−50 kDa and deacetylation degree (DD) of 95% (Heppe Medical Chitosan Gmbh, Halle, Germany), and PAH, M_W = 17,500 g mol^{-1} (Sigma-Aldrich, Steinheim, Germany), were used as polycations. Chi is not soluble in ultrapure water. Therefore, Chi solution was obtained by first

https://doi.org/10.1021/acs.langmuir.2c00191
Langmuir 2022, 38, 5579−5589

dissolving 50 mg of Chi in approximately 25 mL of ultrapure water and 60 μL of HCl 3.7% at 60 °C for 1 h. Then, pH was adjusted with NaOH 10 M and the volume was brought to exactly 100 mL. Finally, the Chi solution was filtered with a 5 and 0.2 μm filters to remove small impurities. Ultrapure water was always used (Elga Purelab Chorus 1, 18.2 MΩ cm, Veolia, United Kingdom). The ionic strength was kept as low as possible, with only the ions necessary for pH adjustment brought in the solutions. It was equal to 1.8 and 0.25 mM at pH 3.5 and 5, respectively, with the pH value measured with a pH-indicator strip (MQuant, Merck, Darmstadt, Germany).

Formation of PPCs. Since electrostatic interactions drive PPCs formation, the PE-to-protein molar ratio in the complexes is usually expressed as the PE-to-protein charge ratio. The charge ratio was calculated as the ratio of PE net charge to the protein net structural charge at a given pH. The PE charge was calculated by the Henderson−Hasselbalch equation (the ionization degree, as a function of pH, was taken into account). For Alg, a pK_a of 3.5 was considered for the carboxylate groups.[55] The pK_a of PAH is approximately 8.5 due to the amine groups.[62] Finally, for Hep and PSS, the sulfonate groups were considered as fully negatively charged. The protein charge was determined using the PDB2PQR server.[63] It was computed as a function of pH, based on their amino acid sequence and on their structure (PDB files of, respectively, 2K6O for LL-37, 3I40 for Ins, 1HEL for Lyz, and 1GAL for Gox). PPCs were prepared from solutions at $I \approx 0$ mM obtained by adding NaOH or HCl to ultrapure water until the desired pH was reached. Proteins were used below their IEP and associated with a polyanion, or conversely, they were used above their IEP and complexed with a polycation. PPCs at a (−)/(+net) charge ratio of 2 were prepared by mixing 2 volumes of a negatively charged PE solution (0.5 mM negative charge) with 5 volumes of a protein solution (0.1 mM net positive charge) and PPCs at a (+)/(−net) charge ratio of 2 were prepared by mixing 2 volumes of a positively charged PE solution (0.5 mM positive charge) with 5 volumes of a protein solution (0.1 mM net negative charge). Therefore, the protein and PE concentrations, in the PPCs with a charge ratio of 2, are, respectively, 0.07 and 0.14 mM positive or negative net charge. For optical density measurements, the negative or positive PE solution was always added to the protein solution in such a way that (−)/(+net) or (+)/(−net) charge ratio varied between 0 and 2, e.g., 0.4 mL of negative or positive PE solution was added to 1 mL of protein solution to reach a (−)/(+net) or (+)/(−net) charge ratio of 2.

Optical Density Measurement. Buchhammer et al. have shown that the optical density can be related to the concentration, size, and polydispersity of the PPCs.[64] Importantly, our group has also demonstrated that the optical density measurement can be used to estimate the charge ratio at which the protein charge is over-compensated by the added PE. This informs on the charge ratio (or molar ratio) necessary to obtain PPCs that can be LbL assembled. In the following, optical density measurements were thus used to monitor PPCs formation as a PE is added to the protein solution.[65] The optical density at λ = 450 nm (A_{450}) of the suspension was measured at pH 3.5, 5, or 7.5, depending on the PPCs system, using a UV−vis spectrophotometer (DU800, Beckman Coulter, USA). The A_{450} values were normalized by the dilution factor according to the Beer−Lambert law. Measurements were all performed at 25 °C and were made in triplicate.

Multilayer Construction. Multilayers were constructed by successive adsorption steps. For all experiments, two bilayers of a positively or negatively charged PE (Chi, PAH, or Hep) alternately adsorbed with a negatively or positively charged PE (Alg, Hep, high molar mass PSS_h, M_W = 70,000 g mol^{-1}, Sigma-Aldrich, Steinheim, Germany or PAH) were constructed from PE solutions (0.5 g L^{-1}). Then, two different multilayers were built on this anchoring layer: bare proteins or PPCs, assembled with oppositely charged PEs. Each of these multilayers is formed of five successive bilayers. The following solutions were used: Chi or PAH (0.5 g L^{-1}), Hep, Alg or PSS_l (0.5 g L^{-1}) and LL-37, Ins, Lyz or Gox bare molecules (0.07 mM positive or negative net charge), as well as PPCs suspensions prepared as described in the Formation of PPCs section. Depending on the experimental conditions, the pH of solutions was adjusted to 3.5, 5, or 7.5 with NaOH or HCl.

Quartz Crystal Microbalance with Dissipation Monitoring (QCM-D). The successive adsorption steps described in the Multilayer Construction section were monitored using QCM-D. 4.95 MHz AT-cut gold-coated quartz sensors (Q-sense, Stockholm, Sweden). The sensors were washed in H_2O_2/H_2SO_4 1:3 (v:v), successively rinsed with water and ethanol, and finally exposed to UV-Ozone (UVO Cleaner 42-220, Jelight Company, Irvine, USA). Then, they were mounted in fluid cells (Q-sense E4 system, Q-Sense, Stockholm, Sweden). The solution flow rate and the temperature were, respectively, set at 20 μL min^{-1} and 20 °C. Each adsorption step was followed by a rinsing step of 10 min with ultrapure water adjusted to the same pH. The frequency and dissipation shifts were recorded for the third to eleventh overtones, and the results for the seventh are presented here. The total mass adsorbed on QCM-D crystals (μg cm^{-2}) was computed using the Sauerbrey equation: $\Delta m = -\Delta f_7\ C\ 7^{-1}$, where Δm is the shift of adsorbed mass (ng cm^{-2}), Δf_7 is the frequency shift measured for the seventh overtone (Hz), C is the mass sensitivity constant (ng cm^{-2} Hz^{-1}), and 7 is the overtone number.

RESULTS AND DISCUSSION

Formation of PPCs. PEs are water-soluble polymers containing ionizable groups that provide them with a positive or negative charge, depending on pH. Thanks to their charged nature, these polymers can interact with proteins to form soluble or insoluble complexes. Protein and PE concentration, ionization degree, charge distribution, hydrophobicity, ionizable group nature, and molecular weight all influence PPCs formation.[66,67] The first part of this work aims at investigating the complexation of LL-37, Ins, Lyz, and Gox with Alg, PPS_l, Hep, and PAH in ultrapure water adjusted to a given pH (3.5, 5, or 7.5). In particular, we aim at determining the PE-to-protein charge ratio that will allow the subsequent successful LbL assembly of the PPCs with PEs.

At pH 3.5 and 5, all proteins used have a positive net charge. When the pH increases to pH 7.5, Ins and Gox switch to a negative net charge while LL-37 and Lyz are still positively charged (Figure S1). Therefore, all proteins were complexed with a polyanion at pH 3.5 and 5 while Ins and Gox were complexed with a polycation at pH 7.5. Figure 1 shows an example of PPCs formation, here by mixing Lyz with Hep. The conditions used for PPCs formation are summarized in Table 1.

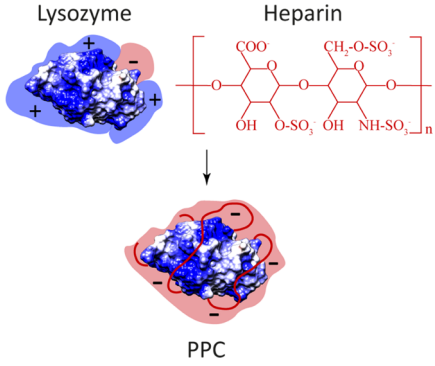

Figure 1. Schematic representation of Lyz-Hep complex formation. Hep is negative and represented by red lines. Lyz is a polyampholyte with the surface potential resulting from positive and negative residues, respectively, colored in blue and red (at pH 3.5). The molecular structure and the surface potential coloring were produced using the UCSF Chimera package.[68]

https://doi.org/10.1021/acs.langmuir.2c00191
Langmuir 2022, 38, 5579−5589

Table 1. Solution pH as a Function of the Protein and the PE Used to Form PPCs

	LL-37	Ins	Lyz	Gox
Alg	pH 5	pH 3.5	pH 5	pH 3.5
PSS_l	pH 5	pH 3.5	pH 5	pH 3.5
Hep	pH 3.5	pH 3.5	pH 3.5	pH 3.5
PAH	x	pH 7.5	x	pH 7.5

A_{450} as a function of PE-to-protein charge ratio is presented in Figures 2a and S2−S5. In all cases, the optical density increases as the PE is added to the protein solution until it reaches a plateau.[65] This optical density plateau, i.e., the charge ratio threshold value beyond which the optical density does not increase, allows the PE-to-protein charge ratio *e* to be determined. This ratio can be related to the minimal amount of PE needed to fully displace the equilibrium toward PPCs formation (Figure 2a). This suggests that, beyond this value, all proteins are in PPCs with a core-corona structure with a neutral internal domain and a PE-charged corona.[69] In a view to further alternate the adsorption of PPCs with an oppositely charged PE, knowing this *e* value is essential. Indeed, once the *e* value is reached, the overall PPCs charge is dictated by the excess of charge brought by the PE (either positive or negative).[70] The measured *e* values for LL-37, Ins, Lyz, and Gox complexed with Hep at pH 3.5, Ins and Gox complexed with Alg and PSS_l at pH 3.5, and finally LL-37 and Lyz complexed with Alg and PSS_l at pH 5 are summarized in Figure 2b.

For all pairs, the *e* value is found between 0.5 and 1.75. Interestingly, PPCs made with Alg, PSS_l, and Hep have, respectively lower, intermediate, and higher *e* values. The *e* value thus scales with the PE charge density. Indeed, for high-charge-density PE such as Hep, all ionizable groups of the PE are unlikely to match and pair with those of the protein. Consequently, an excess of negative charges is needed to fully compensate the protein charge. Though the latter scaling is consistent through all protein−PE pairs, the nature of the protein has the most influence on the *e* absolute value. At a given pH, from low to high, the *e* value order is the following: Gox, LL-37, Lyz, Ins. There is thus no relationship between the *e* value and protein size (see Figure S6 for the size comparison). Using the Chimera software, the protein charge density and distribution at pH 3.5 were computed and are represented in Figure S6. For LL-37, Ins, Lyz, and Gox, the net charges at pH 3.5 are, respectively, equal to +10.4, +3.6, +13.4, and +37.4, and at pH 5, they are, respectively, equal to +7.02, +0.7, +10.5, and +2.9. The charges are homogeneously distributed on the Ins, Lyz, and Gox molecules, whereas LL-37 has a large positive domain.

The complexation of a protein with a net negative charge and a positively charged PE was then studied. At pH 7.5, Ins and Gox have negative net charges of, respectively, −2.1 and −23.1. They were complexed with PAH. The optical density was measured as a function of the effective (+)/(−net) charge ratio. Results are shown in Figure S7. For both Ins and Gox, complexed with PAH, the *e* value equals 2. As for positively charged proteins, these results show that negatively charged proteins can be complexed with PE.

These results show that all proteins could be complexed with a PE by carefully computing their charge at a given pH and selecting the appropriate PE. Moreover, we found that, while protein size does not influence charge overcompensation, the latter scales with the PE charge density and the nature of the protein. PPCs charge overcompensation is critical to standardize the protein charge and facilitate its self-assembly in an LbL fashion.[49] These results will thus be used to identify the appropriate molar ratio to form PPCs to construct a multilayer by alternate adsorption of the latter with a second PE.

Protein−Polyelectrolyte Layer-by-Layer Assembly. In the following, PPCs formed with various proteins and PEs at a (−)/(+net) or (+)/(−net) charge ratio of 2 were LbL assembled with oppositely charged PEs. The LbL assembly of bare protein with PE, i.e., the classical LbL assembly, was carried out for comparison. The same PE as the one used above to complex the protein was alternately adsorbed with the

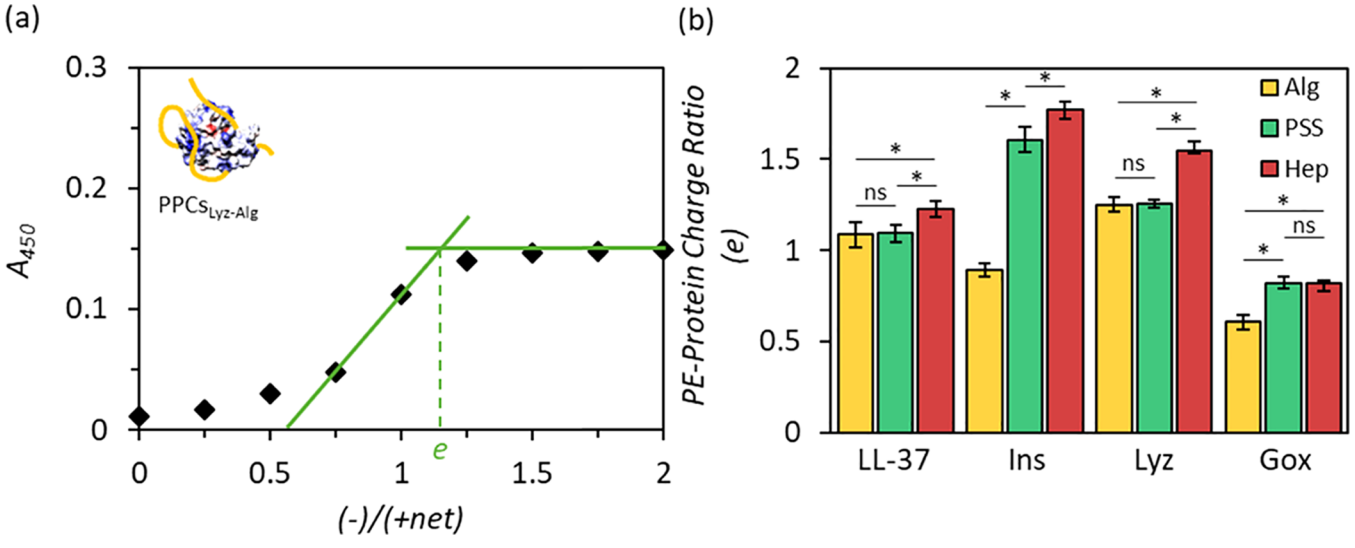

Figure 2. (a) Normalized A_{450} values of a Lyz solution undergoing Alg addition in such a way that (−)/(+net) charge ratio varies between 0 and 2 at pH 5 in ultrapure water (I = 0 mM). *e* represents the charge ratio at which all proteins charges are complexed. (b) (−)/(+net) PE-to-protein charge ratio at which the plateau is reached as an Alg, Hep, or PSS_l solution is added to an LL-37, Ins, Lyz, or Gox solution in ultrapure water. LL-37 and Lyz were complexed at pH 5 with Alg and PSS_l solutions, and the others were complexed at pH 3.5. The error bars represent the standard error (n = 3), and the asterisks indicate a statistically significant difference of the PE-to-protein charge ratio *e* ($p < 0.05$).

https://doi.org/10.1021/acs.langmuir.2c00191
Langmuir 2022, 38, 5579−5589

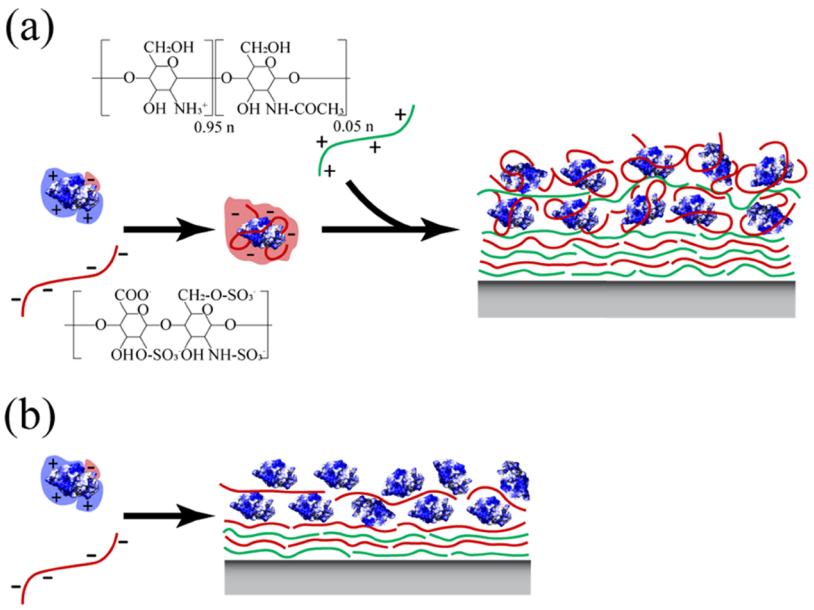

Figure 3. Schematic of the two different methods used to immobilize Lyz. The red and green lines represent, respectively, Hep and Chi. The different colors on Lyz suggest its heterogeneous charge distribution. First, a cushion of two Chi-Hep bilayers was adsorbed on the surface. Then, (a) $PPCs_{Lyz\text{-}Hep}$ were adsorbed using Chi as the positive counter polyion and (b) bare Lyz was adsorbed, using Hep as the negative counter polyion, in a classical LbL assembly.

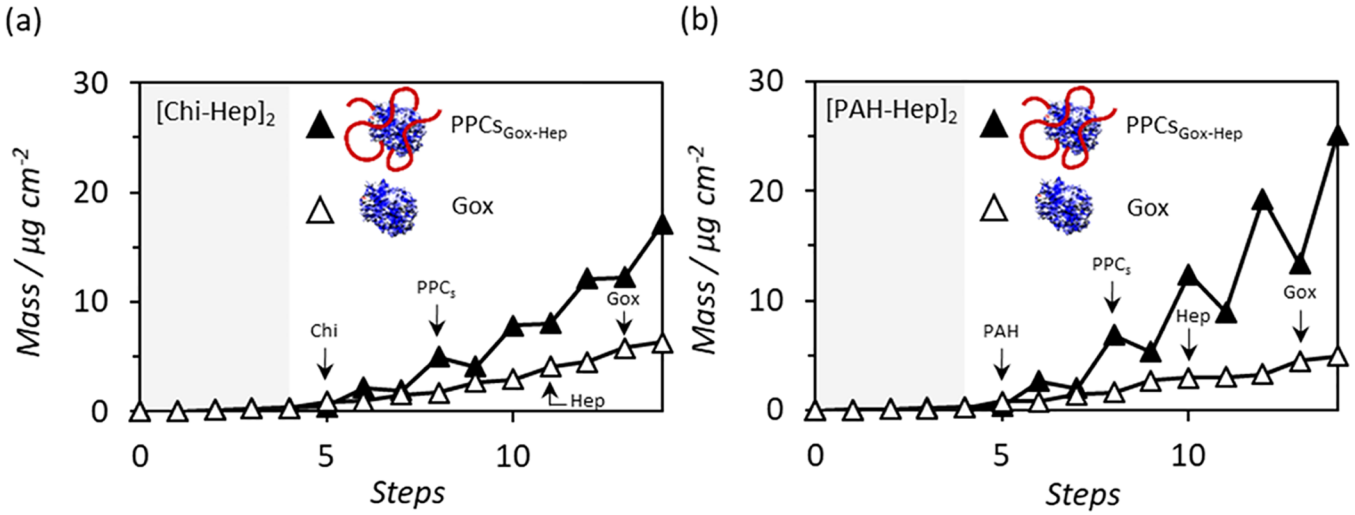

Figure 4. (a) Adsorbed mass measured by QCM-D after the adsorption of a bilayer of Chi-Hep ($[Chi\text{-}Hep]_2$) (shaded area) followed by five bilayers of Chi and either Gox-based PPCs (plain triangle) $[Chi\text{-}PPCs_{Gox\text{-}Hep}]_5$ or bare Gox proteins (empty triangle) $[Gox\text{-}Hep]_5$, at pH 3.5 in ultrapure water. (b) Adsorbed mass measured by QCM-D after the adsorption of a bilayer of PAH-Hep ($[PAH\text{-}Hep]_2$) (shaded area) followed by five bilayers of PAH and either Gox-based PPCs (plain triangle) $[PAH\text{-}PPCs_{Gox\text{-}Hep}]_5$ or bare Gox proteins (empty triangle) $[Gox\text{-}Hep]_5$, at pH 3.5 in ultrapure water.

bare protein molecule to form a multilayer. Figure 3 shows a schematic of films made with Lyz complexed with Hep or bare Lyz molecules assembled with, respectively, Chi and Hep. In all cases, two bilayers of PEs were constructed to screen the effect of the surface.[49] This cushion is made of the PE used to integrate the PPCs in the multilayer and the PE used to complex the protein of interest. Then, five bilayers of PPCs or bare proteins and PEs were constructed. The multilayer growth was monitored using QCM-D, and the results are expressed in adsorbed mass as a function of each adsorption step for each protein−PE combination (Figures S8−S13—see Experimental Section for details on the mass measurement). The adsorbed mass is calculated at the end of each adsorption step, when the steady state is reached. Figures S14−S26 demonstrate that this equilibrium is reached at the end of each deposition step and of each rinsing step. Figures S14−S26 represent the evolution of the frequency and dissipation as a function of time. They support the validity of the use of the Sauerbrey equation to compute mass deposition from frequency shifts.

A typical result is shown in Figure 4 for Gox complexed with Hep ($PPCs_{Gox\text{-}Hep}$) and assembled with Chi ($[Chi\text{-}PPCs_{Gox\text{-}Hep}]$) or PAH ($[PAH\text{-}PPCs_{Gox\text{-}Hep}]$), and for Gox bare molecules assembled with Hep ($[Gox\text{-}Hep]$). In this case, the classical LbL assembly $[Gox\text{-}Hep]$ on either a $[Chi\text{-}Hep]$ or a $[PAH\text{-}Hep]$ bilayer cushion led to an increase of mass of, respectively, 6 $\mu g\ cm^{-2}$ (Figure 4a) and 5 $\mu g\ cm^{-2}$ (Figure 4b)

https://doi.org/10.1021/acs.langmuir.2c00191
Langmuir 2022, 38, 5579−5589

after deposition of five bilayers on the cushion. When $PPCs_{Gox\text{-}Hep}$ are assembled with Chi or PAH, the mass increased by, respectively, 17 and 25 $\mu g\ cm^{-2}$ after five bilayers (Figure 4). This result confirms that PPCs with a (−)/(+net) charge ratio of 2 can be used to build multilayers. It also suggests that these PPCs are negatively charged since they can self-assemble with a polycation. Interestingly, a sawtooth adsorption profile is observed for the [PAH-$PPCs_{Gox\text{-}Hep}$] multilayer. At each $PPCs_{Gox\text{-}Hep}$ adsorption step, the total mass increases, while at each PAH adsorption step, the total mass decreases. These results suggest that material is removed from the multilayer upon PAH adsorption. From these results, we find that (1) the multilayer mass after five layers of protein deposition and (2) the magnitude of the desorption upon PE adsorption can inform the growth of a selected system. These data will thus be extracted from QCM-D results and discussed hereunder for all of the multilayers that were fabricated.

For each of the 32 different self-assembled films that were built, the multilayer masses after five PPCs or bare proteins adsorption steps were extracted and are presented as heat map in Figure S27. To better capture the mass difference, i.e., the improved protein adsorption when PPCs are used, the mass increase compared to classical LbL assembly was computed for each protein−PE combination. Results are presented in Figure 5 and show the mass increase in percent for each of the 16 protein−PE couples tested. From these results, it appears that except for Ins and one condition with Lyz ([Chi-$PPCs_{Lyz\text{-}Hep}$]), all multilayers grow to higher masses when using PPCs rather than bare protein molecules. These results confirm that PPCs can be used to immobilize a wide variety of proteins and PEs in multilayers. Interestingly, the total adsorbed mass scales with the molecular weight of proteins for both types of self-assemblies and most of the protein−PE combinations. Since all PEs used are identical and adsorption is carried out in identical pH and I conditions, this suggests that the mass difference is due to the presence of protein in the multilayer or a difference in the multilayer architecture, e.g., more water in the film. Therefore, the mass difference could be interpreted as an increased protein adsorption or a more hydrated multilayer when PPCs are used compared to bare protein molecules. Both are of great interest since it has been shown that the biological activity increases with the increase in protein concentration[71] and a higher hydrated film can improve the biological activity of proteins. Importantly, our previous works showed that $PPCs_{Lyz\text{-}PAH}$ immobilize Lyz that have 75% more enzymatic activity than bare Lyz molecules.[48,49]

For the multilayers integrating [Chi-$PPCs_{LL\text{-}37\text{-}Hep}$] and [LL-37-Hep], the ratio between the dissipation shift ΔD and the frequency shift Δf obtained for the seventh overtone ($\Delta D_7/(-\Delta f_7/7)$) were calculated. These QCM-D measurements are presented in Figure 6a. Ratios calculated at the beginning, when the cushion is adsorbed, are inconstant because dissipation and frequency shifts are both very low and close to zero (data not shown). Ratios obtained during the adsorption of PPCs and bare proteins are below the value of $\Delta D_7/(-\Delta f_7/7) = 4 \times 10^{-7}\ Hz^{-1}$, proposed by Reviakine et al. as the threshold between rigid and soft films.[72] Figure 6b represents, for the 16 studied systems, the $\Delta D_7/(-\Delta f_7/7)$ difference between the PPCs and the bare protein multilayers after the third adsorption step of PPCs. For all of the systems, ratios are greater when PPCs are integrated into the multilayers than bare proteins. This suggests that multilayers with PPCs are more hydrated than the multilayers with bare proteins.

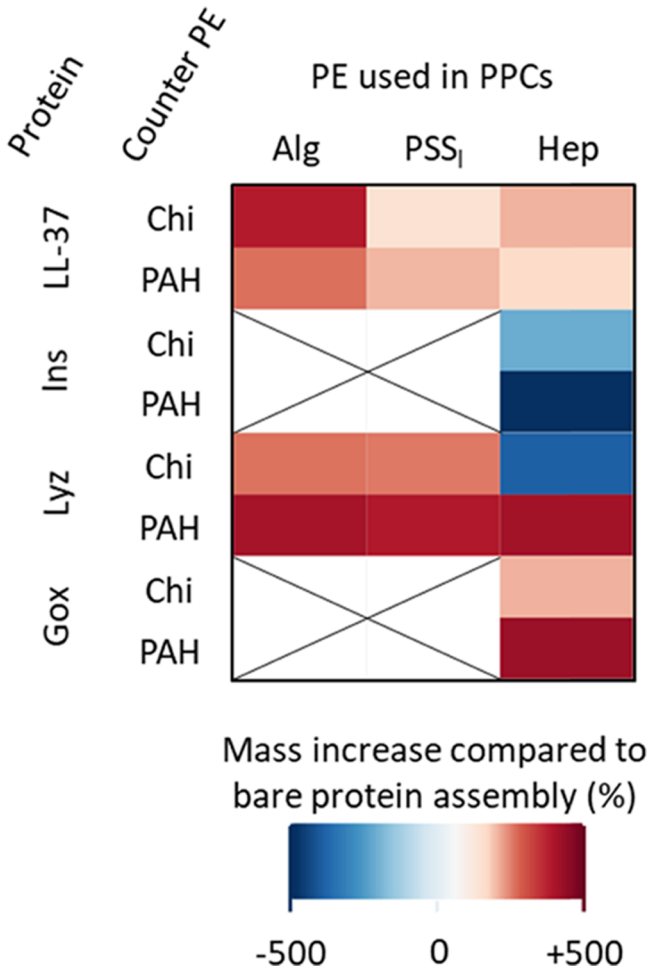

Figure 5. Heat map representing the mass increase when PPCs are used compared to bare proteins. Results with PPCs are expressed in percent of the total mass adsorbed after adsorption of a two bilayers cushion and five adsorption steps of PEs and bare proteins.

The second parameter that was extracted from the multilayer growth is the magnitude of desorption upon PE adsorption. This value was expressed as a percent of the multilayer mass and represented as heat map for each LbL assembly in Figure 7. Interestingly, these results show that desorption is almost systematically observed upon PAH adsorption on a layer of PPCs. On the contrary, Chi adsorption never causes desorption. Desorption is thus observed when a PE with a high charge density is adsorbed on a PPCs layer. On the other hand, no decrease in mass is observed when a PE with a low charge density such as Chi is used (less ionizable groups per unit of length, deacetylation degree of 95%, and lower pK_a). When it comes to the difference between proteins, the adsorption of PAH on a PPCs layer that contains Lyz or Gox leads to a stronger desorption than when it is adsorbed on a PPCs layer that contains LL-37. The desorption is thus less pronounced with a protein that has a high charge density, such as LL-37 (Figures S8−S13). We have recently demonstrated that PPCs-based multilayers are highly dynamic self-assemblies. In particular, we have shown that when a PE is adsorbed on a PPCs layer, it can complex the PE of the PPCs, which releases the protein and causes a decrease of the multilayer mass.[73] Similar phenomena have

https://doi.org/10.1021/acs.langmuir.2c00191
Langmuir 2022, 38, 5579−5589

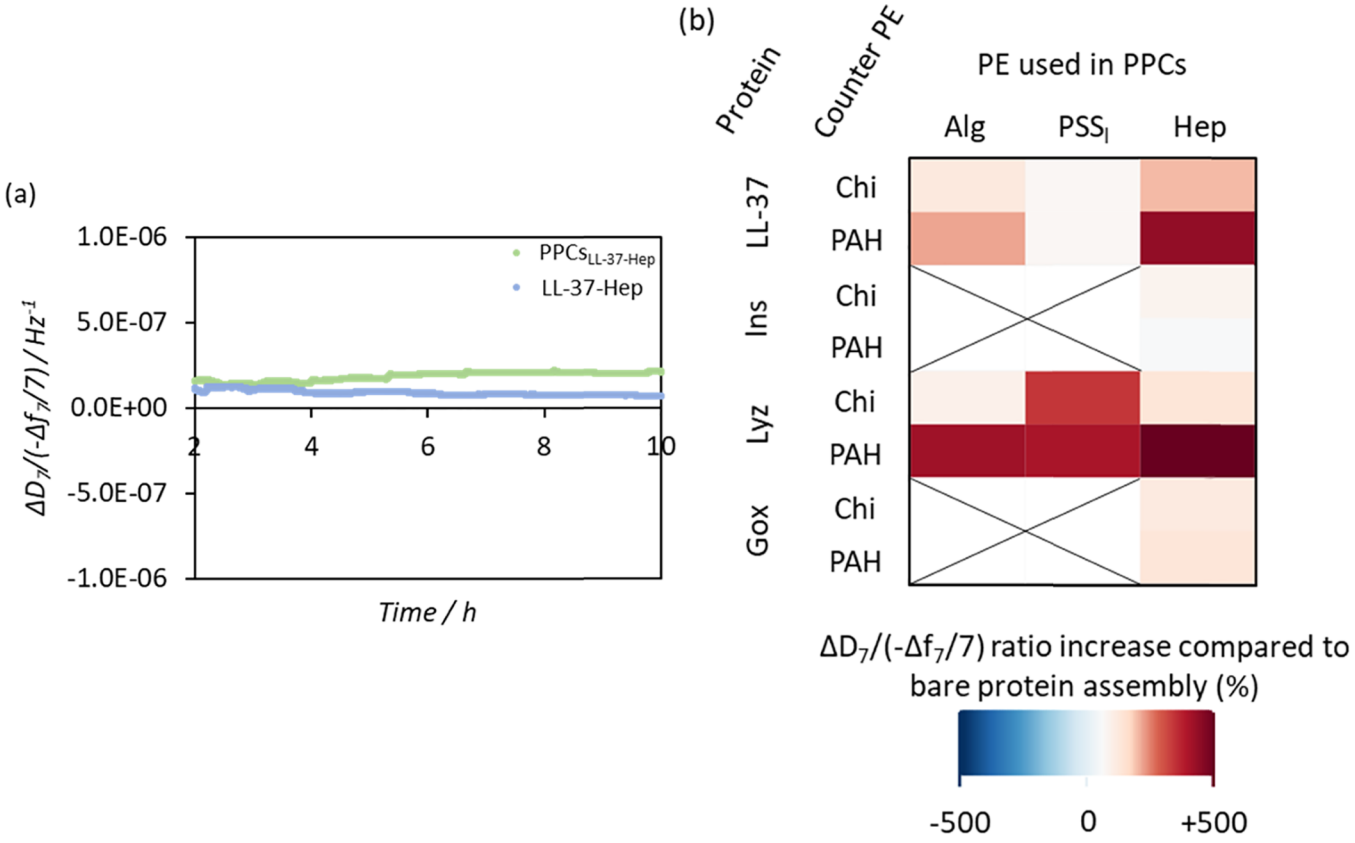

Figure 6. (a) Typical ratios between ΔD_7 and Δf_7 obtained under the adsorption steps using the QCM-D. (b) Heat map representing the $\Delta D_7/(-\Delta f_7/7)$ ratio increase when PPCs are used compared to bare proteins. Results with PPCs are expressed in percent of the $\Delta D_7/(-\Delta f_7/7)$ ratio of bare protein assembly, after the third adsorption step of the PPCs.

been reported in PEMs, especially for systems containing small molecules, where typical stepwise curves in a sawtooth profile (adsorption−desorption steps) were observed.[74] In a previous study, we suggested that this mechanism is a function of the PE−PE ion-pairing strength compared to the protein−PE pairing strength.[73] This hypothesis is in line with the difference in desorption observed for PAH compared to Chi, and for LL-37 compared to Ins and Gox. Indeed, PAH has a strong ion pairing with Alg, PSS_I, and Hep; hence, it can displace proteins from PPCs. Since LL-37 has a higher charge density than Ins and Gox, its pairing with Alg, PSS_I, and Hep is stronger. The result is that PAH adsorption displaces less LL-37 from the PPCs than Ins and Gox. Our results thus confirm that the desorption from the multilayer is the result of a trade-off between PE−PE and protein−PE pairing strengths.

The stability of multilayers to environmental conditions was also investigated. To do so, QCM-D and XPS measurements were performed, by submitting $[Chi\text{-}Hep]_2$-$[Chi\text{-}PPCs_{LL\text{-}37\text{-}Hep}]_6$ samples to a Mueller Hinton Broth (MHB), NaCl (pH 9 and I = 150 mM), or sodium dodecyl sulfate (SDS) solution. QCM-D analyses enable to account for potential desorption of the films due to contact of the multilayers with the solutions and the XPS analyses inform whether the surface chemical composition of the films is modified or not after such contact. Contact of $[Chi\text{-}Hep]_2$-$[Chi\text{-}PPCs_{LL\text{-}37\text{-}Hep}]_6$ multilayer with NaCl and SDS solutions leads to a mass loss attributed to partial desorption of the film (data not shown). It could suggest a film deconstruction due to a change in pH and I.[75,76] The XPS analysis of Ti 2p peaks indicates that a partial but not complete film desorption has occurred (Figure S28). No mass increase or decrease was observed after the immersion of the film in the MHB solution, suggesting a higher stability of the multilayer in this medium. By analyzing N 1s and C 1s XPS peaks (Figure S28), it seems that the effect of sample treatment with a solution of MHB and NaCl on the surface elemental composition is relatively limited. Indeed, there is almost no difference in comparison with the untreated $[Chi\text{-}PPCs_{LL\text{-}37\text{-}Hep}]_6$ sample. However, the addition of SDS modified the multilayer composition, indicating desorption of the film and suggesting adsorption of SDS molecules on the surface of the sample. Rahim et al. also observed desorption of [PAH-PSS] PEMs upon the addition of SDS, which was proven to be chemically adsorbed into the multilayers.[77] Therefore, the stability of LbL films is found to be highly dependent on the medium and the PEs.

To further study the LbL assembly of PPCs, multilayers were built using positively charged PPCs. To do so, $PPCs_{Ins\text{-}PAH}$ and $PPCs_{Gox\text{-}PAH}$ were integrated into multilayers with Hep at pH 7.5. The total masses after five bare proteins or PPCs adsorption steps were extracted and are presented in Figure S29. From these results, it appears that the multilayers does not grow when PPCs are used even though the PPCs are well formed (Figure S7). On the contrary, a multilayer constructed with bare Ins and Gox, respectively, reaches masses of 0.7 and 1.8 $\mu g\ cm^{-2}$. This difference can be explained by the use of PAH and Hep as PEs. As shown before, the PE−PE ion-pairing strength dictates the multilayer growth. For this system, Hep has the highest charge density that exists among natural PEs.[58] Thus, it seems that Hep is able to displace Gox and Ins from the PPCs. However, we do not

https://doi.org/10.1021/acs.langmuir.2c00191
Langmuir 2022, 38, 5579−5589

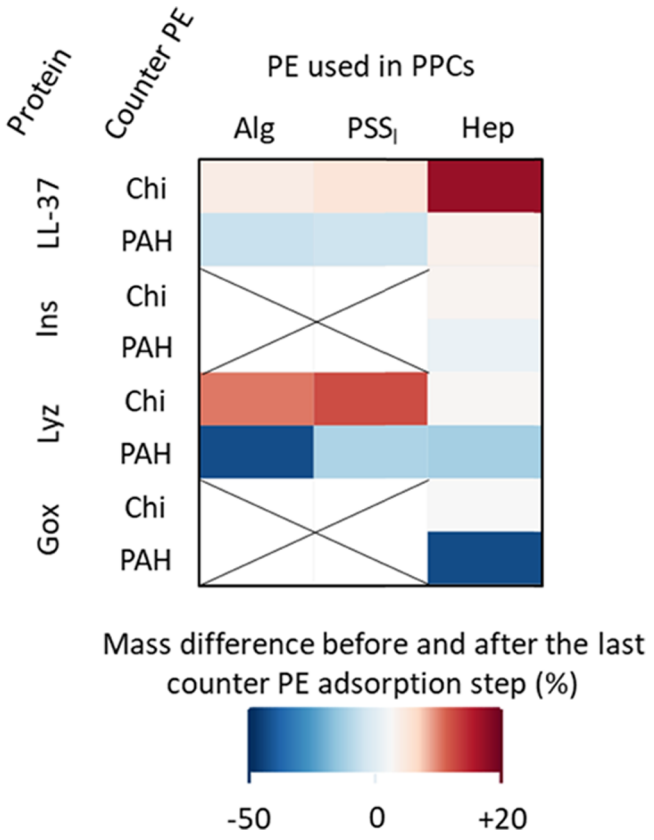

Figure 7. Heat map representing the desorption (blue) and the adsorption (red) into the multilayer after the last Chi or PAH adsorption step. Results are expressed in percent of the total mass adsorbed before the last addition of Chi or PAH.

explain this by the lack of charge of PAH, which is not fully ionized at pH 7.5 since we constructed multilayers of PPCs$_{Lyz\text{-}PSSl}$ integrated with PAH at pH 7.5.[48,49] Studies, more focused on the interactions between these species, should be conducted to understand the nonconstruction of multilayers when proteins are complexed with PAH.

We have thus shown that the difference between films integrating PPCs and those integrating bare proteins is noteworthy. The use of PPCs leads to an increase, by up to 4 times, of the protein mass and/or the hydration in the multilayer. Importantly, the PEs need to be carefully selected to avoid their pairing and subsequent protein release from the film. Once this is accounted for, PPCs can be used as a more generalizable tool for protein surface immobilization.

PPCs Layer-by-Layer Assembly to Combine Different Proteins. To date, the studied systems included only one type of protein. The immobilization of several proteins at interfaces to create multifunctional multilayers is topical for various fields of research as drug release, tissue engineering, and regenerative medicine approaches.[78] The purpose of studying the assembly of PPCs based on different types of proteins is twofold. First, the possibility of incorporating several proteins, independently of each other, will be analyzed. Second, the parameters governing this integration will be compared to the ones of bare proteins. To do so, the assembly of mixed layers based on PPCs$_{LL\text{-}37\text{-}Alg}$ and PPCs$_{LL\text{-}37\text{-}PSSl}$, as well as on PPCs$_{Lyz\text{-}Alg}$ and PPCs$_{Lyz\text{-}PSSl}$ was monitored. The PPCs, which are negatively charged, were integrated with PAH at pH 5. The total masses after five PPCs or bare proteins adsorption steps (three with LL-37 and two with Lyz) were extracted from QCM-D data and are presented in Figure 8. Regarding the classical LbL assemblies that integrate LL-37 and Lyz, with either Alg or PSS$_l$, no building of the layers was observed. For Alg-based PPCs and PSS$_l$-based PPCs assembled with PAH, the mass increased by, respectively, 2 and 1.4 μg cm^{-2} after five bilayers. These results suggest that the multilayers grow to higher masses when using PPCs rather than bare protein molecules. As was the case for multilayers with a single type of proteins, dissipation values (data not shown) indicate that PPCs-based films are more hydrated. Similarly, a desorption step was

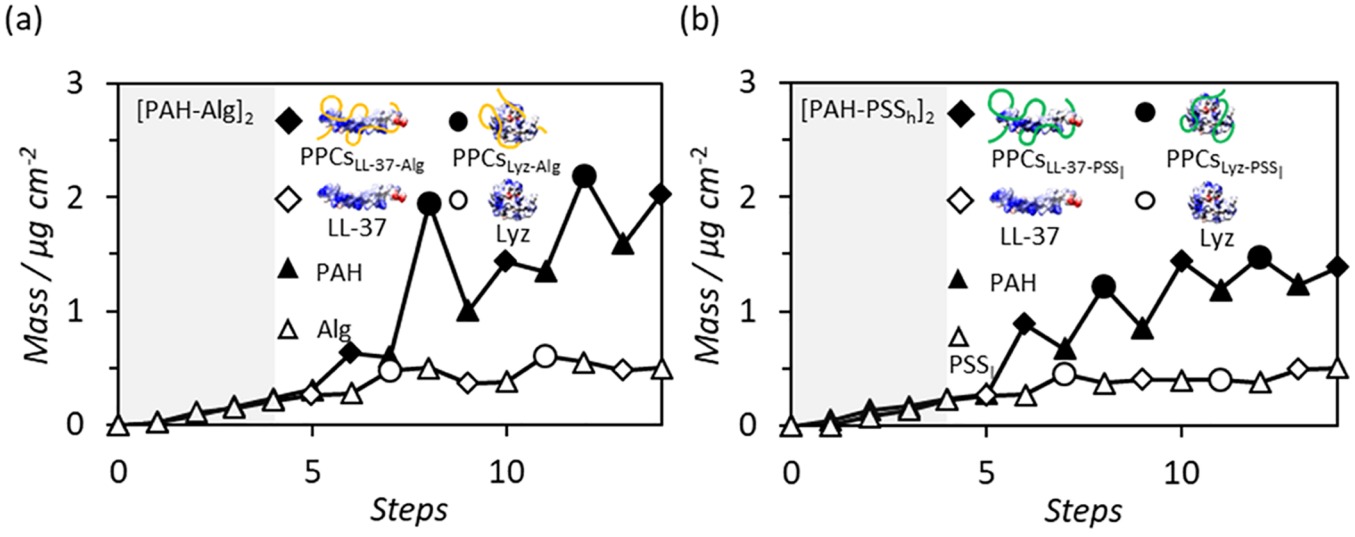

Figure 8. (a) Adsorbed mass measured by QCM-D after the adsorption of a bilayer of PAH-Alg ([PAH-Alg]$_2$) (shaded area) followed by either five bilayers of PAH (plain triangle), three of PPCs$_{LL\text{-}37\text{-}Alg}$ (plain square) and two of PPCs$_{Lyz\text{-}Alg}$ (plain circle), or five bilayers of Alg (empty triangle), three of bare LL-37 (empty square) and two of bare Lyz (empty circle), at pH 5 in ultrapure water. (b) Adsorbed mass measured by QCM-D after the adsorption of a bilayer of PAH-PSS$_h$ ([PAH-PSS$_h$]$_2$) (shaded area) followed by either five bilayers of PAH (plain triangle), three of PPCs$_{LL\text{-}37\text{-}PSSl}$ (plain square) and two of PPCs$_{Lyz\text{-}PSSl}$ (plain circle), or five bilayers of PSS$_l$ (empty triangle), three of bare LL-37 (empty square) and two of bare Lyz (empty circle), at pH 5 in ultrapure water.

https://doi.org/10.1021/acs.langmuir.2c00191
Langmuir 2022, 38, 5579−5589

systematically observed upon PAH adsorption on PPCs layers. Interestingly, the nature of the selected molecules guides again dictates the film growth. Indeed, for the Alg-based PPCs, a greater mass is adsorbed with $PPCs_{Lyz}$ than with $PPCs_{LL\text{-}37}$ and the magnitude of desorption upon PAH adsorption is larger with $PPCs_{Lyz}$ than with $PPCs_{LL\text{-}37}$, which stabilizes very quickly. This result is in line with that observed when a single type of protein was self-assembled into multilayers (Figures S10 and S11). The trend is also maintained for both the PSS_l-based PPCs types (Figures S12 and S13). These results highlight that it is possible to integrate several types of proteins by PPCs self-assemblies within the same multilayer. However, the PE and the protein in the PPCs as well as the counter PE largely influence the multilayer formation. Depending on the species involved in the multilayers, the adsorption profile is quite different.

CONCLUSIONS

In this paper, we demonstrated that PPCs are versatile building blocks for the LbL assembly of proteins. PPCs were obtained by complexation of LL-37, Ins, Lyz, and Gox with Alg, PSS_l, Hep, and PAH. We showed that the PE-to-protein charge ratio *e*, i.e., the minimal amount of PE needed to fully displace the equilibrium toward PPCs formation, is reached at a charge ratio below 2 for all of them. PPCs with a PE-to-protein charge ratio of 2 were then assembled into multilayers using Chi, PAH, and Hep. Compared to the use of bare protein molecules, using PPCs generally allows a better multilayer growth, ranging from two to four times higher mass. We show that this difference in mass is due to a higher hydration level of multilayers integrating PPCs and/or a higher mass of proteins. Finally, we evidenced that the nature of the protein and PE of the PPCs, and the nature of the counter PE used to build the films play a key role in the ability to self-assemble. Indeed, protein−PE and PE−PE pairing strengths are critical in that respect.

Such self-assembled PPCs are thus promising as versatile building blocks since it is possible to fine-tune the nature of the multilayer and therefore potentially its functionality. PPCs are of major importance for the development of bioactive interphases since they provide a higher protein and/or hydration level than the use of bare proteins.

ASSOCIATED CONTENT

Supporting Information

The Supporting Information is available free of charge at https://pubs.acs.org/doi/10.1021/acs.langmuir.2c00191.

Protein net charge as a function of the solution pH, turbidimetry measurements, protein molecular structure, surface charge organization and density, evolution of the adsorbed mass upon multilayer buildup by QCM-D, evolution of the frequency and dissipation shifts upon multilayer buildup by QCM-D, heat map of multilayer total mass, and XPS analyses (PDF)

AUTHOR INFORMATION

Corresponding Authors

Cédric Vranckx − *Institute of Condensed Matter and Nanosciences, Bio- and Soft Matter, Université catholique de Louvain, B-1348 Louvain-la-Neuve, Belgium;* orcid.org/0000-0003-3833-0067; Email: cedric.vranckx@uclouvain.be

Christine Dupont-Gillain − *Institute of Condensed Matter and Nanosciences, Bio- and Soft Matter, Université catholique de Louvain, B-1348 Louvain-la-Neuve, Belgium;* orcid.org/0000-0002-6153-4044; Email: christine.dupont@uclouvain.be

Authors

Laure Lambricht − *Louvain Drug Research Institute, Advanced Drug Delivery and Biomaterials, Université catholique de Louvain, 1200 Brussels, Belgium*

Véronique Préat − *Louvain Drug Research Institute, Advanced Drug Delivery and Biomaterials, Université catholique de Louvain, 1200 Brussels, Belgium*

Olivier Cornu − *Neuro-Musculo-Skeletal Pole, Experimental and Clinical Research Institute and Orthopaedic and Trauma Department, Cliniques Universitaires Saint-Luc, Université catholique de Louvain, 1200 Brussels, Belgium*

Aurélien vander Straeten − *Institute of Condensed Matter and Nanosciences, Bio- and Soft Matter, Université catholique de Louvain, B-1348 Louvain-la-Neuve, Belgium;* orcid.org/0000-0002-5435-1987

Complete contact information is available at: https://pubs.acs.org/10.1021/acs.langmuir.2c00191

Notes

The authors declare no competing financial interest.

ACKNOWLEDGMENTS

This work was supported by the Belgian National Fund for Scientific Research (FNRS) and the Training Fund for Research in Industry and Agriculture (FRIA). The authors are grateful to the anonymous referees for comments that have been very helpful for improving the initial version of the present work.

REFERENCES

(1) Han, C.; Guo, W. Fluorescent Noble Metal Nanoclusters Loaded Protein Hydrogel Exhibiting Anti-Biofouling and Self-Healing Properties for Electrochemiluminescence Biosensing Applications. *Small* **2020**, *16*, No. 2002621.

(2) Teanphonkrang, S.; Schulte, A. Automated Quantitative Enzyme Biosensing in 24-Well Microplates. *Anal. Chem.* **2017**, *89*, 5261−5269.

(3) Büscher, N.; Sayoga, G. V.; Rübsam, K.; Jakob, F.; Schwaneberg, U.; Kara, S.; Liese, A. Biocatalyst Immobilization by Anchor Peptides on an Additively Manufacturable Material. *Org. Process Res. Dev.* **2019**, *23*, 1852−1859.

(4) Zhang, G.; Johnston, T.; Quin, M. B.; Schmidt-Dannert, C. Developing a Protein Scaffolding System for Rapid Enzyme Immobilization and Optimization of Enzyme Functions for Biocatalysis. *ACS Synth. Biol.* **2019**, *8*, 1867−1876.

(5) Schoeller, J.; Itel, F.; Wuertz-Kozak, K.; Gaiser, S.; Luisier, N.; Hegemann, D.; Ferguson, S. J.; Fortunato, G.; Rossi, R. M. PH-Responsive Chitosan/Alginate Polyelectrolyte Complexes on Electrospun PLGA Nanofibers for Controlled Drug Release. *Nanomaterials* **2021**, *11*, No. 1850.

(6) Lu, Y.; Aimetti, A. A.; Langer, R.; Gu, Z. Bioresponsive Materials. *Nat. Rev. Mater.* **2016**, *2*, No. 16075.

(7) Kitsara, M.; Tassis, G.; Papagiannopoulos, A.; Simon, A.; Agbulut, O.; Pispas, S. Polysaccharide−Protein Multilayers Based on Chitosan−Fibrinogen Assemblies for Cardiac Cell Engineering. *Macromol. Biosci.* **2022**, *22*, No. 2100346.

(8) Zander, N. E.; Orlicki, J. A.; Rawlett, A. M.; Beebe, T. P. Quantification of Protein Incorporated into Electrospun Polycapro-

lactone Tissue Engineering Scaffolds. *ACS Appl. Mater. Interfaces* **2012**, *4*, 2074−2081.
(9) Richardson, J. J.; Björnmalm, M.; Caruso, F. Technology-Driven Layer-by-Layer Assembly of Nanofilms. *Science* **2015**, *348*, 411−422.
(10) Faccio, G. From Protein Features to Sensing Surfaces. *Sensors* **2018**, *18*, No. 1204.
(11) Roach, P.; Farrar, D.; Perry, C. C. Interpretation of Protein Adsorption: Surface-Induced Conformational Changes. *J. Am. Chem. Soc.* **2005**, *127*, 8168−8173.
(12) Li, T.; Hao, L.; Li, J.; Du, C.; Wang, Y. Insight into Vitronectin Structural Evolution on Material Surface Chemistries: The Mediation for Cell Adhesion. *Bioact. Mater.* **2020**, *5*, 1044−1052.
(13) Jain, A.; Trindade, G. F.; Hicks, J. M.; Potts, J. C.; Rahman, R.; Hague, R. J. M.; Amabilino, D. B.; Pérez-García, L.; Rawson, F. J. Modulating the Biological Function of Protein by Tailoring the Adsorption Orientation on Nanoparticles. *J. Colloid Interface Sci.* **2021**, *587*, 150−161.
(14) Yong, K. W.; Yuen, D.; Chen, M. Z.; Porter, C. J. H.; Johnston, A. P. R. Pointing in the Right Direction: Controlling the Orientation of Proteins on Nanoparticles Improves Targeting Efficiency. *Nano Lett.* **2019**, *19*, 1827−1831.
(15) Latour, R. A. Fundamental Principles of the Thermodynamics and Kinetics of Protein Adsorption to Material Surfaces. *Colloids Surf., B* **2020**, *191*, No. 110992.
(16) Norde, W.; Buijs, J.; Lyklema, H. Adsorption Of Globular Proteins. *Fundam. Interface Colloid Sci.* **2005**, *5*, 3.1−3.59.
(17) Langmuir, I.; Schaefer, V. J. Properties and Structure of Protein Monolayers. *Chem. Rev.* **1939**, *24*, 181−202.
(18) Weltz, J. S.; Kienle, D. F.; Schwartz, D. K.; Kaar, J. L. Reduced Enzyme Dynamics upon Multipoint Covalent Immobilization Leads to Stability-Activity Trade-Off. *J. Am. Chem. Soc.* **2020**, *142*, 3463−3471.
(19) Ogorzalek, T. L.; Wei, S.; Liu, Y.; Wang, Q.; Brooks, C. L.; Chen, Z.; Marsh, E. N. G. Molecular-Level Insights into Orientation-Dependent Changes in the Thermal Stability of Enzymes Covalently Immobilized on Surfaces. *Langmuir* **2015**, *31*, 6145−6153.
(20) Decher, G.; Hong, J. D.; Schmitt, J. Buildup of Ultrathin Multilayer Films by a Self-Assembly Process: III. Consecutively Alternating Adsorption of Anionic and Cationic Polyelectrolytes on Charged Surfaces. *Thin Solid Films* **1992**, *210−211*, 831−835.
(21) Schlenoff, J. B.; Ly, H.; Li, M. Charge and Mass Balance in Polyelectrolyte Multilayers. *J. Am. Chem. Soc.* **1998**, *120*, 7626−7634.
(22) Decher, G. Fuzzy Nanoassemblies: Toward Layered Polymeric Multicomposites. *Science* **1997**, *277*, 1232−1237.
(23) Hammond, P. T. Recent Explorations in Electrostatic Multilayer Thin Film Assembly. *Curr. Opin. Colloid Interface Sci.* **1999**, *4*, 430−442.
(24) Borges, J.; Mano, J. F. Molecular Interactions Driving the Layer-by-Layer Assembly of Multilayers. *Chem. Rev.* **2014**, *114*, 8883−8942.
(25) Ariga, K.; Lvov, Y.; Decher, G. There Is Still Plenty of Room for Layer-by-Layer Assembly for Constructing Nanoarchitectonics-Based Materials and Devices. *Phys. Chem. Chem. Phys.* **2022**, *24*, 4097−4115.
(26) Kleinfeld, E. R.; Ferguson, G. S. Stepwise Formation of Multilayered Nanostructural Films from Macromolecular Precursors. *Science* **1994**, *265*, 370−373.
(27) de Lucena, N. C.; Miyazaki, C. M.; Shimizu, F. M.; Constantino, C. J. L.; Ferreira, M. Layer-by-Layer Composite Film of Nickel Phthalocyanine and Montmorillonite Clay for Synergistic Effect on Electrochemical Detection of Dopamine. *Appl. Surf. Sci.* **2018**, *436*, 957−966.
(28) Lvov, Y.; Hass, H.; Decher, G.; Möhwald, H.; et al.*et al.* Successive Deposition of Alternate Layers of Polyelectrolytes and a Charged Virus. *Langmuir* **1994**, *10*, 4232−4236.
(29) Watanabe, S.; Regen, S. L. Dendrimers as Building Blocks for Multilayer Construction. *J. Am. Chem. Soc.* **1994**, *116*, 8855−8856.
(30) Yoshida, K.; Yamaguchi, A.; Midorikawa, H.; Kamijo, T.; Ono, T.; Dairaku, T.; Sato, T.; Fujimura, T.; Kashiwagi, Y.; Sato, K. Adsorption and Release of Rose Bengal on Layer-by-Layer Films of Poly(Vinyl Alcohol) and Poly(Amidoamine) Dendrimers Bearing 4-Carboxyphenylboronic Acid. *Polymers* **2020**, *12*, 1854.
(31) Jiang, Y.; Shen, Y.; Wu, P. Self-Assembly of Multilayer Films Containing Gold Nanoparticles via Hydrogen Bonding. *J. Colloid Interface Sci.* **2008**, *319*, 398−405.
(32) Yuehui, W.; Xing, Y. High-Reflection Optical Thin Films Based on SiO2/TiO2 Nanoparticles Multilayers by Dip Coating. *Micro Nano Lett.* **2018**, *13*, 1349−1351.
(33) Lvov, Y.; Decher, G.; Sukhorukov, G. Assembly of Thin Films by Means of Successive Deposition of Alternate Layers of DNA and Poly(Allylamine). *Macromolecules* **1993**, *26*, 5396−5399.
(34) Mauquoy, S.; Dupont-Gillain, C. Combination of Collagen and Fibronectin to Design Biomimetic Interfaces: Do These Proteins Form Layer-by-Layer Assemblies? *Colloids Surf., B* **2016**, *147*, 54−64.
(35) Delechiave, G.; Naves, A. F.; Kolanthai, E.; da Silva, R. A.; Vlasman, R. C.; Petri, D. F. S.; Torresi, R. M.; Catalani, L. H. Tuning Protein Delivery from Different Architectures of Layer-by-Layer Assemblies on Polymer Films. *Mater. Adv.* **2020**, *1*, 2043−2056.
(36) Lvov, Y.; Ariga, K.; Ichinose, I.; Kunitake, T. Assembly of Multicomponent Protein Films by Means of Electrostatic Layer-by-Layer Adsorption. *J. Am. Chem. Soc.* **1995**, *117*, 6117−6123.
(37) Vigier-Carrière, C.; Garnier, T.; Wagner, D.; Lavalle, P.; Rabineau, M.; Hemmerlé, J.; Senger, B.; Schaaf, P.; Boulmedais, F.; Jierry, L. Bioactive Seed Layer for Surface-Confined Self-Assembly of Peptides. *Angew. Chem., Int. Ed.* **2015**, *54*, 10198−10201.
(38) Rodon Fores, J.; Martinez Mendez, M. L.; Mao, X.; Wagner, D.; Schmutz, M.; Rabineau, M.; Lavalle, P.; Schaaf, P.; Boulmedais, F.; Jierry, L. Localized Supramolecular Peptide Self-Assembly Directed by Enzyme-Induced Proton Gradients. *Angew. Chem., Int. Ed.* **2017**, *56*, 15984−15988.
(39) Vigier-Carrière, C.; Wagner, D.; Chaumont, A.; Durr, B.; Lupattelli, P.; Lambour, C.; Schmutz, M.; Hemmerlé, J.; Senger, B.; Schaaf, P.; et al. Control of Surface-Localized, Enzyme-Assisted Self-Assembly of Peptides through Catalyzed Oligomerization. *Langmuir* **2017**, *33*, 8267−8276.
(40) Rodon Fores, J.; Criado-Gonzalez, M.; Chaumont, A.; Carvalho, A.; Blanck, C.; Schmutz, M.; Serra, C. A.; Boulmedais, F.; Schaaf, P.; Jierry, L. Supported Catalytically Active Supramolecular Hydrogels for Continuous Flow Chemistry. *Angew. Chem., Int. Ed.* **2019**, *58*, 18817−18822.
(41) Silva, R. A.; Urzúa, M. D.; Petri, D. F. S.; Dubin, P. L. Protein Adsorption onto Polyelectrolyte Layers: Effects of Protein Hydrophobicity and Charge Anisotropy. *Langmuir* **2010**, *26*, 14032−14038.
(42) Becker, A. L.; Henzler, K.; Welsch, N.; Ballauff, M.; Borisov, O. Proteins and Polyelectrolytes: A Charged Relationship. *Curr. Opin. Colloid Interface Sci.* **2012**, *17*, 90−96.
(43) Sukhishvili, S. A.; Kharlampieva, E.; Izumrudov, V. Where Polyelectrolyte Multilayers and Polyelectrolyte Complexes Meet. *Macromolecules* **2006**, *39*, 8873−8881.
(44) Ariga, K.; Onda, M.; Lvov, Y.; Kunitake, T. Alternate Layer-by-Layer Assembly of Organic Dyes and Proteins Is Facilitated by Pre-Mixing with Linear Polyions. *Chem. Lett.* **1997**, *26*, 25−26.
(45) Jin, W.; Shi, X.; Caruso, F. High Activity Enzyme Microcrystal Multilayer Films. *J. Am. Chem. Soc.* **2001**, *123*, 8121−8122.
(46) Xia, J.; Dubin, P. Protein-Polyelectrolyte Complexes. In *Macromolecular Complexes in Chemistry and Biology*; Dubin, P.; Bock, J.; Davis, R.; Schulz, D. N.; Thies, C., Eds.; Springer: Berlin, Heidelberg, 1994; pp 247−271.
(47) Cooper, C. L.; Dubin, P. L.; Kayitmazer, A. B.; Turksen, S. Polyelectrolyte−Protein Complexes. *Curr. Opin. Colloid Interface Sci.* **2005**, *10*, 52−78.
(48) vander Straeten, A.; Bratek-Skicki, A.; Germain, L.; D'Haese, C.; Eloy, P.; Fustin, C.-A.; Dupont-Gillain, C. Protein−Polyelectrolyte Complexes to Improve the Biological Activity of Proteins in Layer-by-Layer Assemblies. *Nanoscale* **2017**, *9*, 17186−17192.
(49) vander Straeten, A.; Bratek-Skicki, A.; Jonas, A. M.; Fustin, C.-A.; Dupont-Gillain, C. Integrating Proteins in Layer-by-Layer Assemblies Independently of Their Electrical Charge. *ACS Nano* **2018**, *12*, 8372−8381.

https://doi.org/10.1021/acs.langmuir.2c00191
Langmuir 2022, 38, 5579−5589

(50) Vandamme, D.; Landuyt, B.; Luyten, W.; Schoofs, L. A Comprehensive Summary of LL-37, the Factoctum Human Cathelicidin Peptide. *Cell. Immunol.* **2012**, *280*, 22−35.
(51) Comune, M.; Rai, A.; Palma, P.; TondaTuro, C.; Ferreira, L. Antimicrobial and Pro-Angiogenic Properties of Soluble and Nanoparticle-Immobilized LL37 Peptides. *Biomater. Sci.* **2021**, *9*, 8153−8159.
(52) Chipman, D. M.; Grisaro, V.; Sharon, N. The Binding of Oligosaccharides Containing N-Acetylglucosamine and N-Acetylmuramic Acid to Lysozyme. The Specificity of Binding Subsites. *J. Biol. Chem.* **1967**, *242*, 4388−4394.
(53) Vermassen, A.; Leroy, S.; Talon, R.; Provot, C.; Popowska, M.; Desvaux, M. Cell Wall Hydrolases in Bacteria: Insight on the Diversity of Cell Wall Amidases, Glycosidases and Peptidases toward Peptidoglycan. *Front. Microbiol.* **2019**, *10*, No. 331.
(54) Wang, Z.; Liu, S.; Wu, P.; Cai, C. Detection of Glucose Based on Direct Electron Transfer Reaction of Glucose Oxidase Immobilized on Highly Ordered Polyaniline Nanotubes. *Anal. Chem.* **2009**, *81*, 1638−1645.
(55) Haug, A. *Composition and Properties of Alginates*; Report No. 30, Norwegian Institute of Seaweed Research: Trondheim, Norway, 1964; p 123.
(56) Sun, J.; Tan, H. Alginate-Based Biomaterials for Regenerative Medicine Applications. *Materials* **2013**, *6*, 1285−1309.
(57) Xu, M.; Qin, M.; Cheng, Y.; Niu, X.; Kong, J.; Zhang, X.; Huang, D.; Wang, H. Alginate Microgels as Delivery Vehicles for Cell-Based Therapies in Tissue Engineering and Regenerative Medicine. *Carbohydr. Polym.* **2021**, *266*, No. 118128.
(58) Salmivirta, M.; Lidholt, K.; Lindahl, U. Heparan Sulfate: A Piece of Information. *FASEB J.* **1996**, *10*, 1270−1279.
(59) Domard, A. PH and c.d. Measurements on a Fully Deacetylated Chitosan: Application to CuII—Polymer Interactions. *Int. J. Biol. Macromol.* **1987**, *9*, 98−104.
(60) Li, J.; Zhuang, S. Antibacterial Activity of Chitosan and Its Derivatives and Their Interaction Mechanism with Bacteria: Current State and Perspectives. *Eur. Polym. J.* **2020**, *138*, No. 109984.
(61) Castleberry, S. A.; Almquist, B. D.; Li, W.; Reis, T.; Chow, J.; Mayner, S.; Hammond, P. T. Self-Assembled Wound Dressings Silence MMP-9 and Improve Diabetic Wound Healing in Vivo. *Adv. Mater.* **2016**, *28*, 1809−1817.
(62) Choi, J.; Rubner, M. F. Influence of the Degree of Ionization on Weak Polyelectrolyte Multilayer Assembly. *Macromolecules* **2005**, *38*, 116−124.
(63) Dolinsky, T. J.; Nielsen, J. E.; McCammon, J. A.; Baker, N. A. PDB2PQR: An Automated Pipeline for the Setup of Poisson-Boltzmann Electrostatics Calculations. *Nucleic Acids Res.* **2004**, *32*, W665−W667.
(64) Buchhammer, H. M.; Mende, M.; Oelmann, M. Preparation of Monodisperse Polyelectrolyte Complex Nanoparticles in Dilute Aqueous Solution. *Prog. Colloid Polym. Sci.* **2004**, *124*, 98−102.
(65) Kayitmazer, A. B.; Seeman, D.; Minsky, B. B.; Dubin, P. L.; Xu, Y. Protein-Polyelectrolyte Interactions. *Soft Matter* **2013**, *9*, 2553−2583.
(66) Seyrek, E.; Dubin, P. L.; Tribet, C.; Gamble, E. A. Ionic Strength Dependence of Protein-Polyelectrolyte Interactions. *Biomacromolecules* **2003**, *4*, 273−282.
(67) Gao, S.; Holkar, A.; Srivastava, S. Protein − Polyelectrolyte Complexes and Micellar Assemblies. *Polymers* **2019**, *11*, 1097.
(68) Pettersen, E. F.; Goddard, T. D.; Huang, C. C.; Couch, G. S.; Greenblatt, D. M.; Meng, E. C.; Ferrin, T. E. UCSF Chimera - A Visualization System for Exploratory Research and Analysis. *J. Comput. Chem.* **2004**, *25*, 1605−1612.
(69) Cousin, F.; Gummel, J.; Combet, S.; Boué, F. The Model Lysozyme-PSSNa System for Electrostatic Complexation: Similarities and Differences with Complex Coacervation. *Adv. Colloid Interface Sci.* **2011**, *167*, 71−84.
(70) Amaduzzi, F.; Bomboi, F.; Bonincontro, A.; Bordi, F.; Casciardi, S.; Chronopoulou, L.; Diociaiuti, M.; Mura, F.; Palocci, C.; Sennato, S. Chitosan-DNA Complexes: Charge Inversion and DNA Condensation. *Colloids Surf., B* **2014**, *114*, 1−10.
(71) Gupta, A. Enzymes. In *Comprehensive Biochemistry for Dentistry*; Springer: Singapore, 2019; pp 185−205.
(72) Reviakine, I.; Johannsmann, D.; Richter, R. P. Hearing What You Cannot See and Visualizing What You Hear. *Anal. Chem.* **2011**, *83*, 8838−8848.
(73) vander Straeten, A.; Dupont-Gillain, C. Self-Reorganizing Multilayer to Release Free Proteins from Self-Assemblies. *Langmuir* **2020**, *36*, 972−978.
(74) Cheng, M.; Jiang, C.; Luo, C.; Zhang, Y.; Shi, F. Investigating Zigzag Film Growth Behaviors in Layer-by-Layer Self-Assembly of Small Molecules through a High-Gravity Technique. *ACS Appl. Mater. Interfaces* **2015**, *7*, 18824−18831.
(75) Hoogeveen, N. G.; Cohen Stuart, M. A.; Fleer, G. J.; Böhmer, M. R. Formation and Stability of Multilayers of Polyelectrolytes. *Langmuir* **1996**, *12*, 3675−3681.
(76) Dubas, S. T.; Farhat, T. R.; Schlenoff, J. B. Multiple Membranes from "True" Polyelectrolyte Multilayers. *J. Am. Chem. Soc.* **2001**, *123*, 5368−5369.
(77) Rahim, M. A.; Choi, W. S.; Lee, H. J.; Jeon, I. C. Ionic Surfactant-Triggered Renewal of the Structures and Properties of Polyelectrolyte Multilayer Films. *Langmuir* **2010**, *26*, 4680−4686.
(78) Casanova, M. R.; Reis, R. L.; Martins, A.; Neves, N. M. Surface Biofunctionalization to Improve the Efficacy of Biomaterial Substrates to Be Used in Regenerative Medicine. *Mater. Horiz.* **2020**, *7*, 2258−2275.

https://doi.org/10.1021/acs.langmuir.2c00191
Langmuir 2022, 38, 5579−5589